Research Square

Preprints are preliminary reports that have not undergone peer review.
They should not be considered conclusive, used to inform clinical practice,
or referenced by the media as validated information.

Endothelial Cell Activation by Interleukin-1 and Extracellular Matrix Laminin-10 Occurs via the Yap Signalling Pathway

Hannah Thurgur
The University of Manchester
Jeffrey Penny
The University of Manchester
Emmanuel Pinteaux (emmanuel.pinteaux@manchester.ac.uk)
The University of Manchester https://orcid.org/0000-0002-9986-4401

Research Article

Keywords: extracellular matrix, laminin, inflammation, brain endothelia, interleukin, angiogenesis

Posted Date: April 2nd, 2021

DOI: https://doi.org/10.21203/rs.3.rs-365829/v1

License: This work is licensed under a Creative Commons Attribution 4.0 International License.
Read Full License

Abstract

Background: The extracellular matrix (ECM) plays an important role for normal brain functions and homeostasis, and contributes to the inflammatory response and mechanisms of brain repair after acute brain injury. We have previously reported that the ECM laminin-10 (LM-10) is a key regulator of blood-brain barrier (BBB) integrity, and is involved in BBB repair after hypoxic injury and interleukin-1 (IL-1)-induced inflammation *in vitro*. To further investigate the role of LM-10 in BBB inflammation and repair, we investigated for the first time the signalling mechanisms regulated by LM-10 in brain endothelial cells in response to IL-1β-induced inflammation *in vitro*.

Methods: Human brain endothelial cell line hCMEC/D3 cultured on Matrigel- or LM-10-coated tissue culture plates were left untreated or were treated with human recombinant IL-1β at various concentrations and/or for various periods of time. *In vitro* hallmarks of angiogenesis were assessed using a scratch injury model and tube formation assay. Expression of cell adhesion molecules ICAM-1 and VCAM-1, as well as IL-8 was measured using ELISA. Activation of signalling pathways ERK1/2, p38, NF-κB and YAP was assessed by quantitative ELISA or Western blot. Activation of genes downstream of YAP signalling was assessed by quantitative polymerase chain reaction.

Results: LM-10 promoted endothelial proliferation and subsequent repair of an endothelial monolayer after scratch injury, induced tube formation, and upregulated IL-1β-induced ICAM-1 and VCAM-1 expression *in vitro*. Classical IL-1β-induced signalling pathway ERK1/2 and p38 were not modulated by LM-10, whilst LM-10 upregulated IL-1β-induced NF-κB activation. Importantly, we demonstrate for the first time a role of the YAP signalling pathway in endothelial cell activation, in that LM-10 significantly downregulates p-YAP (S397) activation without affecting phosphorylation of YAP (S127), leading to differential expression of YAP target genes, *ctgf* and *serpine-1* involved in endothelial cell activation.

Conclusion: Our study provides for the first time evidence that the YAP signalling pathway is an important regulator of endothelial cell activation, and could be a new therapeutic target for the treatment of cerebrovascular inflammatory diseases.

Introduction

In physiological conditions, the extracellular matrix (ECM) of the central nervous system (CNS) provides a structural and functional environment for the cells of the neurovascular unit that is essential for maintenance of blood-brain barrier (BBB) integrity and brain homeostasis. However, after cerebral ischaemia, the BBB undergoes profound changes associated with the breakdown of tight junctions, remodelling of the ECM and enzymatic degradation of ECM proteins [1,2]. The early events of BBB breakdown are also associated with leukocyte infiltration, mediated by cell adhesion molecules and chemokines [3]. The cytokine interleukin(IL)-1 is an established mediator of the pro-inflammatory response associated with BBB dysfunction and subsequent tissue damage [4]. Although IL-1 is known to exert detrimental actions during the acute phase of stroke, increasing evidence suggests a biphasic

action of IL-1 that exhibits neuroreparative properties during the sub-acute phase [5]. Furthermore, increasing evidence suggests that the ECM plays a dynamic role during the detrimental phase of stroke, whilst promoting repair during the later stages post-stroke. Interestingly, a novel function of the ECM as a regulator of IL-1-induced signalling in astrocytes and cerebral endothelial activation has been demonstrated *in vitro* [6,7]. ECM remodelling after CNS injury is associated with BBB repair, and IL-1 has been shown to mediate repair mechanisms, leading to the hypothesis that BBB repair driven by IL-1 could be regulated by ECM remodelling. Indeed, we have recently demonstrated LM-10 as a key ECM molecule involved in BBB repair after hypoxic injury and IL-1-induced inflammation *in vitro* [8]. However, the role of LM-10 as a regulator of inflammation and angiogenesis had not yet been determined.

The mechanisms underlying the dynamic crosstalk between the ECM and inflammation are poorly understood. Although it has been previously demonstrated that different components of the ECM alter IL-1 signalling pathways in astrocytes and endothelial cells *in vitro* [6,7], the crosstalk between signalling pathways downstream of the IL-1 receptor and other key signalling pathways has not been fully characterised. The YAP/Hippo pathway has recently gained significant interest as an extremely dynamic pathway implicated in ECM remodelling, as seen in cancer and inflammatory diseases [9,10]. It is well established that ECM-integrin signalling is a key step in the initiation of the YAP pathway. Critically, recent evidence has demonstrated a key role of YAP in tumour necrosis factor-α-induced endothelial activation [11]. However, the role of YAP in endothelial cells after IL-1 treatment had not yet been determined, and whether LM-10 could modulate this response is currently unknown. Using *in vitro* approaches, we demonstrate here that LM-10 modulates key *in vitro* hallmarks of angiogenesis and modulates endothelial cell activation after IL-1β treatment through the upregulation of key adhesion molecules, and demonstrate a novel mechanism whereby YAP signalling pathway is involved in endothelial activation by IL-1β, providing new signalling mechanisms of cerebrovascular activation regulated by IL-1 and the ECM.

Materials And Methods

Tissue culture plate coating

Tissue culture plates (Corning, UK) were coated at 4°C overnight with human recombinant LM-10 (Biolamina, Sweden) diluted in phosphate-buffered saline (PBS) with calcium and magnesium (PBS+) at concentrations of 0.1, 1, 2.5, 5, 10 µg/ml. Control wells were incubated with filter sterilised 0.22 µm pore size filter (Starlab, UK) 0.1 % (w/v) low endotoxin bovine serum albumin (BSA) in PBS^{+}. After overnight incubation, LM-10 solutions were discarded. PBS^{+} was added to control and LM-10 coated wells to prevent drying out. Tissue culture plates were stored at 4 °C. For experiments using Matrigel, neat Matrigel (9.16 mg/ml, Corning) was diluted in Dulbecco's Modified Eagle's Medium (DMEM) (Invitrogen, UK) to a concentration of 20 µg/ml, and tissue culture plates were pre-coated at 4°C overnight. Plates were washed in PBS^{-} before cell seeding.

hCMEC endothelial cell line culture

The immortalised human cerebral microvascular endothelial cell line, hCMEC/D3, was purchased from Merck (UK). Cells were cultured in 75 cm^2 tissue culture flasks pre-coated with rat tail collagen type I (Merck, UK), (1:100 in PBS) at 37 °C for 1 h, and maintained in EndoGRO-MV complete culture media [5% fetal bovine serum, L-glutamine (10 mM), EndoGRO-LS supplement (0.2 %), heparin sulphate (0.75 U/ml), ascorbic acid (50 µg/ml), hydrocortisone hemisuccinate (1 µg/ml), recombinant human epidermal growth factor (5 ng/ml), recombinant human basic fibroblast growth factor (1 ng/ml; Merck) and 1% penicillin-streptomycin] at 37 °C in a humidified atmosphere containing 5 % CO2. Cells were passaged at 80-90% confluency using 0.25 % trypsin/ 1 mM EDTA solution, and were used in experiments until passage 10.

Cell culture treatments

hCMEC/D3 cells were seeded at a density of 200,000 cells/well in 24-well plates pre-coated with Matrigel (20 µg/ml) or LM-10 (10 µg/ml) in EndoGRO-MV complete culture medium for 4 h. For inflammatory mediator release experiments, cultures were treated with recombinant human IL-1β (R&D Systems, UK) at 0.1, 0.3, 1, 3, 10 or 100 ng/ml diluted in EndoGRO-MV complete culture medium, for 24 h. Control cultures were treated with vehicle (EndoGRO-MV complete culture medium alone) for 24 h. For signalling pathway and qPCR experiments, cultures were treated with IL-1β (10 ng/ml) for 5, 15, 30, 60,120 or 240 min.

Enzyme-linked immunosorbent assay (ELISA)

ICAM-1, VCAM-1, phospho-p38a and phospho-ERK1/2 levels in cell lysates, and IL-8 levels in supernatants, were quantified by human ELISA (R&D Systems, UK) according to the manufacturer's instructions. Absorbance was measured at 450 nm and corrected at 570 nm using a plate reader (Synergy HT, BioTek, UK). The standard curve was fitted by a sigmoidal 4PL equation in GraphPad Prism. Concentrations in the samples were calculated by interpolating the values from the standard curve. Levels of all cytokines were corrected for cell number and expressed as pg/ml per µg/ml of total protein (pg/µg of protein), using total protein determined by the BCA assay.

Western blot analyses

hCMEC/D3 cells were lysed in RIPA buffer (50 mM Tris-HCl, 150 mM NaCl, 1% sodium deoxycholate, 0.1% SDS, and 2 mM EDTA) supplemented with 1% protease inhibitor cocktail and phosphatase inhibitors. Lysates were denaturated in Laemmli buffer (2% (w/v) SDS, 5% (v/v) β-mercaptoethanol, 10% (v/v) glycerol in 60mM Tris-HCl, pH 6.8) at 95°C for 5 min, and equal amount of protein were resolved on 10% SDS polyacrylamide gel, then transferred onto polyvinylidene difluoride (Bio-Rad) using a Trans-Blot Turbo Transfer System (Bio-Rad). Non-specific binding sites were blocked with 5% (w/v) BSA in PBS 0.1% (v/v) Tween 20 (PBST) for 1 h at room temperature (RT). Membranes were then incubated (4 °C) overnight in primary antibody in PBST 5% BSA, as follows; anti IκBα (Cell Signalling UK, 1/1000); anti phospho-p65 (Ser536) (Cell Signalling UK, 1/1000); anti p-YAP127 (Cell Signalling UK, 1/1000); anti p-YAP397 (Cell Signalling UK, 1/1000); anti YAP (Cell Signalling UK, 1/1000); anti β-actin (Abcam UK, 1/1000). Membranes were washed in PBST and incubated with secondary anti rabbit anti-IgG (Agilent UK, 1/1000) antibody in PBST 1 % BSA for 1 h at RT. Membranes were washed and incubated in ECL

Prime Western Blotting Detection Reagent (GE Life Sciences, UK) before exposure with G:BOX (Syngene) and Genesys software. Densitometry was determined using ImageJ software, and detected intensities were normalised against β-actin. Finally, ratios of pYAP/YAP were calculated.

Quantitative polymerase chain reaction (qPCR)

RNAs were extracted using Purelink RNA minikit (Thermo Fisher Scientific, UK) according to the manufacturer's instructions, with the use of PureLink™ DNase Set (Thermo Fisher Scientific). Extracted RNAs were assessed for yield and purity using Nanodrop 1000. Messenger RNA (1 µg) was converted to cDNA using SuperScript™ III Reverse Transcriptase (Thermo Fisher Scientific), according to the manufacturer's instructions. Quantitative polymerase chain reaction (qPCR) was performed using Power SYBR Green PCR Master Mix (Thermo Fisher Scientific) in 384-well format using a 7900HT Fast Real-Time PCR System (Applied Biosystems). Three microliters of 1:20 diluted cDNA was loaded with 200 mmol/l of primers in triplicate. Primers used were as follows; Ctgf FWD: CAGCATGGACGTTCGTCTG, REV: AACCACGGTTTGGTCCTTGG; Serpine 1 FWD: ACCGCAACGTGGTTTTCTCA, REV: TTGAATCCCATAGCTGCTTGAAT; GAPDH FWD: GCACCGTCAAGGCTGAGAAC, REV: AGGGATCTCGCTCCTGGAA. Data were normalized to the expression of the housekeeping gene GAPDH. Expression levels of genes of interest were calculated as follows: relative mRNA expression=E−(Ct of gene of interest)/ E−(Ct of housekeeping gene), where Ct is the threshold cycle value and E is efficiency.

Scratch wound assay

hCMEC/D3 cells were seeded at 40,000 cells/well in 96-well ImageLock plate (Essen BioScience) and left to adhere for 4 h. Scratch wound injury was carried out using a 96-pin IncuCyte WoundMaker Tool (Essen BioScience). Cells were then washed twice with PBS and replaced with fresh media. Phase contrast images were acquired at 2 h intervals for a period of 24 h on an Incucyte Zoom Live Cell Analysis system using a 4x/3.05 Plan Apo OFN25 objective. The 96-well Cell Migration Software Application Module (Essen BioScience) was used to quantify relative wound density. Relative wound density is a measure (%) of the density of the wound region relative to the density of the cell region:

$$\%RWD(t) = (w(t)-w(0)) / (c(t)-w(0)) \times 100$$

w(t)=Density of wound region at time, (t)

c(t)=Density of cell region at time, (t)

Tube formation assay

50 µl of undiluted Matrigel (9.16 mg/ml) was added to individual wells of an ice-cold 96-well plates, and the plate incubated at 37 °C for 45 min to allow gelation. 70 µl of either LM-10 (10 µg/ml) or PBS (control) was added to the Matrigel pre-coated wells, and plates were incubated for a further 2 h at 37°C. The PBS and LM-10 aqueous layers on top of the Matrigel were aspirated. hCMEC/D3 cells were resuspended in media supplemented with 3 µg/ml bFGF and were seeded at a density of 10,000

cells/well. Phase contrast images were acquired at 0 and 6.5 h on an Incucyte Zoom Live Cell Analysis system using a 4x/3.05 Plan Apo OFN25 objective. The angiogenesis analyser macro in ImageJ was used to quantify total number of branches and total branching length.

Statistical analyses

All data were analysed with GraphPad Prism 8.1.2 (GraphPad Software Inc) using the statistical tests stated in the figure legends. Homoscedasticity of the standard deviations were evaluated with a Brown-Forsythe and Bartlett's test, alongside the use of homoscedasticity plots (predicted vs residual) and QQ plots to assess equal variance and normality. Appropriate transformations were applied where necessary. Data are presented as mean ± standard error of mean (SEM). Details of replicates are indicated in the figure legend. Statistical significance was accepted at *$p < 0.05$, **$p < 0.01$, ***$p < 0.001$, and ****$p < 0.0001$.

Results

LM-10 regulates angiogenic phenotype and IL-1β-induced activation of hCMEC/D3 cells.

We previously reported that LM-10 plays a key role in the maintenance of BBB integrity, and reverses most of the key hallmarks of BBB dysfunction induced by acute hypoxia and IL-1 [8]. In the current study we have used hCMEC/D3 cells, a cell line that has been extensively characterised as a valid brain endothelial phenotype and used as a model of human BBB function [12]. To confirm the cellular effects of LM-10 on hCMEC/D3 cells, we investigated the effect of LM-10 on angiogenic responses using a scratch assay (Fig. 1A) and tube formation assay (Fig. 1B). LM-10 reduced width of scratch in a time-dependent manner compared to Matrigel (Fig.1Ai), reflective of increased endothelial migration into the scratched region. Specifically, LM-10 increased wound density in hCMEC/D3 cultures at every time-point (4 h (64%, p=0.0404), 8 h (60%, p=0.0006), 12 h (52%, p=0.0001), 16 h (39%, p=0.0001), 20 h (20.7%, p=0.0052) and 24 h (16%, p=0.0293)) measured across the 24 h period compared to corresponding time-points on Matrigel (Fig. 1Aii). In the tube formation assay, LM-10 increased the number of branches (1.35-fold increase, p=0.0263) and total branching length (1.57-fold increase, p=0.0144, Fig. 1Bi and ii) compared to Matrigel, showing that LM-10 increase tube-like structures and their length. These data suggest that LM-10 aids endothelial cell migration, an initial step in the processes of angiogenesis and BBB repair.

We next aimed to examine if LM-10 acts as a regulator of IL-1β-induced endothelial cell activation and IL-1β-induced signalling pathways in hCMEC/D3 cells. IL-1β treatment had a significant effect on ICAM-1 ($p<0.0001$, Fig. 2Ai), VCAM-1 ($p<0.0001$, Fig. 2Aii) and IL-8 ($p<0.0001$, Fig. 2Aiii) expression in a concentration-dependent manner. The ECM had a significant effect on expression of VCAM-1 (p=0.0245, Fig. 2Aii) demonstrating an elevated expression of VCAM-1 in hCMEC/D3 cells when grown on LM-10 compared to Matrigel, whilst a trend towards a statistically different effect of LM-10 on ICAM-1 expression was detected (p=0.0576, Fig. 2Ai). Specifically, LM-10 induced a higher IL-1β-induced expression of ICAM-1 in hCMEC/D3 cells treated with IL-1β at 100 ng/ml (1.16 fold, p=0.0089) and VCAM-1 at 10 ng/ml (1.17 fold, p=0.0058), 30 ng/ml (1.16 fold, p=0.0013) and 100 ng/ml (1.22 fold,

p<0.0001) compared to corresponding IL-1β concentrations on Matrigel. No significant effect of ECM coating on IL-8 expression was observed (p=0.6916, Fig. 2Aiii), suggesting that LM-10 does not influence IL-8 expression in hCMEC/D3.

We next investigated whether LM-10 alters IL-1β signalling pathways, namely ERK1/2, p38 and NF-κB, as those are key signalling elements downstream of IL-1 receptor activation in endothelial cells [3,7]. IL-1β had no significant effect on phospho-ERK1/2 levels in hCMEC/D3 cells on Matrigel and LM-10 after 5 and 15 min of IL-1β treatment, whereas a significant decreased (p=0.0012) in phospho-ERK1/2 levels was detected after 30, 60 and 120 min of IL-1β treatment on both matrices (Fig. 2Bi). Importantly no significant effect of LM-10 on IL-1β-induced phospho-ERK1/2 levels was detected. Furthermore, IL-1β treatment significantly increased (p=0.0002) phospho-p38α levels in a time-dependent manner both on Matrigel and LM-10, with maximum activation detected 30 min after IL-1β treatment followed by a decrease in phospho-p38α levels at 60 and 120 min of IL-1β treatment (Fig. 2Bii). No effect of LM-10 on IL-1β-induced p38α activation was detected. Finally, IL-1β treatment significantly increased (p=0.0002) the levels of phospho-NF-κB p65 in a time-dependent manner in cells on Matrigel and LM-10 (Fig. 2Ci). In hCMEC/D3 cells seeded on Matrigel, a significant increase in phospho-NF-κB p65 levels was detected 5 min after IL-1β treatment compared to baseline (15.5-fold increase, p=0.0002), which dropped slightly but remained significantly elevated at 15 min (11-fold increase, p=0.0081), 30 min (13-fold increase, p=0.0011) and 60 min (11-fold increase, p=0.0063), before markedly decreasing at 120 min and 240 min after IL-1β treatment. In hCMEC/D3 cells seeded on LM-10, a significant increase in phospho-NF-κB p65 levels was detected 5 min after IL-1β treatment compared to baseline (12.8-fold increase, p<0.0001), which slightly dropped but remained significantly elevated at 15 min (8.9-fold increase, p=0.0002) and 30 min (7-fold increase, p=0.0046), before markedly decreasing at 60 min after IL-1β treatment. Interestingly the ECM had a significant effect on phospho-NF-κB p65 levels, with significantly higher levels of phospho-NF-κB p65 observed at 5 min after IL-1β treatment in cells seeded on LM-10 compared Matrigel (1.5-fold increase, p=0.0425).

We next assessed IκBα expression after IL-1β treatment in hCMEC/D3 cells (Fig. 2Cii). There was a marked, significant reduction in IκBα levels in hCMEC/D3 cells seeded on Matrigel after 5 min (84%, p= 0.0021), 30 min (95%, p=0.0001) and 60 min (87%, p=0.0016) after IL-1β treatment. A marked and significant reduction in IκBα levels at 5 min (82%, p=0.0013), 30 min (92%, p=0.0001) and 60 min (88%, p=0.0005) after IL-1β treatment was also observed in hCMEC/D3 cells seeded on LM-10. Although IL-1β treatment (p<0.0001) affected IκBα in a time-dependent manner both on Matrigel and LM-10, no effect of ECM was determined and statistical comparison between corresponding time-points showed no significant differences in IκBα levels were detected in cells on Matrigel and LM-10.

LM-10 regulates YAP signalling after IL-1β-induced activation in hCMEC/D3 cells.

Having demonstrated that not all classical IL-1β downstream signalling pathways were modulated by LM-10, we investigated alternative signalling pathways that may be modulated by LM-10 in IL-1-induced activated endothelial cells. The ECM has been recently implicated as a regulator of the YAP/Hippo

pathway [9], and evidence suggests that inflammation can modulate this signalling mechanism [11]. Therefore, we hypothesised that IL-1 and/or LM-10 alters YAP signalling in endothelial cells. To address this hypothesis, we initially measured the phosphorylation of YAP at S127 (Fig. 3Ai) and S397 (Fig. 3Aii) after IL-1β treatment. These phosphorylation sites play differential roles in YAP signalling whereby p-YAP(S127) induces cytoplasmic retention of YAP [13,14], and p-YAP(S397) creates a phospho-degron motif for proteasomal degradation [15]. The p-YAP(S127)/YAP and p-YAP(S397)/YAP ratios are an indicator of levels of dephosphorylated YAP in the cell that is able to translocate into the nucleus and activate associated genes.

When analysing the p-YAP(S127)/YAP ratio after IL-1β treatment in hCMEC/D3 cells, we found that IL-1β treatment significantly ($p<0.0001$) affected p-YAP(S127) levels in a time-dependent manner in cells on either Matrigel or LM-10 (Fig. 3Ai); In hCMEC/D3 cells seeded on Matrigel, phosphorylation of YAP(S127) significantly decreased at 5 min (54%, p=0.0.164) and 15 min (54%, p=0.0053) compared to baseline levels, to then slowly return to baseline levels at 120 min and 240 min. In cells seeded on LM-10, a significant decrease in p-YAP(S127) was observed at 15 min (46%, p=0.0038), which then returned to baseline levels at 120 min and 240 min. No significant effect of ECM on p-YAP(S127) levels was determined, and no significant differences between Matrigel and LM-10 were observed at each time point after IL-1β treatment. Analysing p-YAP(S397)/YAP ratio after IL-1β treatment found that IL-1β significantly ($p=0.0002$) affected p-YAP(S397) levels in a time-dependent manner both on Matrigel and LM-10 (Fig. 3Aii); When hCMEC/D3 cells were seeded on Matrigel, there was a small, no significant, initial reduction in p-YAP(397) levels at 5 min (35% p=0.7288) and 30 min (15%, p=0.9978) after IL-1β treatment compared to baseline. This was followed by a marked increase in p-YAP(397) levels between 30 min and 240 min after IL-1β treatment, and significant increases were observed at 120 min (2.7-fold increase, $p=0.0063$) and 240 min (4.1-fold increase, $p<0.0001$) compared to baseline. In contrast, the signalling pattern of p-YAP(397) expression in hCMEC/D3 seeded on LM-10 was markedly different to cells on Matrigel, in that, a consistent, significant reduction in p-YAP(397) levels in hCMEC/D3 cells on LM-10 was observed between 15 min and 120 min after IL-1β treatment compared to basal levels, with a significant reduction at 15 min (55%, p=0.0349), 30 min (72%, p=0.0089) and 60 min (69%, p=0.0073), followed a small increase in levels observed at 240 min (36%, p=0.4310). Interestingly, the ECM had a significant ($p=0.0112$) effect on the levels of p-YAP(S397), demonstrating elevated levels of p-YAP(S397) on Matrigel compared to LM-10. On direct comparison between corresponding time points on Matrigel and LM-10, significantly higher levels of p-YAP(397) was observed at 30 min (4.2-fold increase, p=0.0219), 120 min (4.5-fold increase, p=0.0014), 240 min (3.63-fold increase, $p<0.0001$) after IL-1β treatment on Matrigel.

To investigate the nuclear activity of YAP as a transcriptional co-activator, we analysed the mRNA levels of its target genes Ctgf (Fig. 3Bi) and Serpine 1 (Fig. 3Bii). There was a significant marked reduction (97%, p=0.0197) of Ctgf mRNA levels in hCMEC/D3 cells on Matrigel after IL-1β treatment, whilst reduction of Ctgf mRNA levels in cells on LM-10 was marginal and not significant (22%, p=0.6031). On direct comparison of baseline Ctgf mRNA levels between cells on Matrigel and LM-10, there was notably elevated levels on LM-10 (1.6-fold increase, p=0.2515). After IL-1β treatment, there was a significant difference in levels of Ctgf mRNA levels between hCMEC/D3 cells grown on Matrigel and LM-10 (42-fold

increase, p=0.0127). In contrast, we observed a different IL-1β effect on Serpine 1 mRNA expression levels whereby no overall effect of IL-1β was observed, whilst there was a trend towards a significant effect of ECM (p=0.0667), suggesting potentially elevated levels of Serpine 1 mRNA in cells on LM-10.

Discussion

Recent research has demonstrated a novel role of the ECM as a regulator of IL-1-induced endothelial inflammation *in vitro* [7] and LM-10 has been identified as a potential mediator of BBB repair *in vitro* [8]. However, the specific role of LM-10 as a regulator of angiogenesis and IL-1-driven endothelial inflammation *in vitro* remained unknown. Furthermore, the signalling crosstalk between IL-1 and YAP/Hippo signalling in endothelial cells has not been investigated. Here we present novel evidence of a dynamic cross-talk between IL-1β and YAP signalling in endothelial cells regulated by LM-10, providing a potential mechanism underlying cerebrovascular inflammatory responses regulated by ECM remodelling in CNS diseases.

Extensive evidence suggests that the ECM plays a dynamic role in CNS repair, providing a supportive framework and contributing to recovery [16]. Indeed, laminins have been shown to be protective against neuronal loss and contribute to neuronal survival [17]. Here we first show that LM-10 increased endothelial proliferation and migration, as well as formation of tube-like structures of hCMEC/D3 in cultures, all hallmarks that have been previously demonstrated to be indicative of angiogenesis [18–20]. However, we further demonstrate a novel function of LM-10 whereby endothelial attachment to LM-10 increases IL-1β-induced ICAM-1 and VCAM-1 expression in hCMEC/D3 cells, further confirming that LM-10 may play an important inflammatory modulatory effect. Indeed, after cerebral ischaemia, ICAM-1 and VCAM-1, key vascular adhesion molecules, are upregulated in brain blood vessels, which aid leukocyte infiltration into the brain and contribute to subsequent tissue injury [4]. Our observation therefore suggest a dual nature of LM-10 during the acute detrimental and subacute reparative phase of injury. Interestingly, VEGF upregulates ICAM-1 brain microvascular endothelial cells [19], mediating their migration, whilst *in vivo* data show that ICAM-1 knockout mice display attenuated VEGF-mediated angiogenesis [21], suggesting that ICAM-1 plays a key role in pathological angiogenesis. There is similar evidence demonstrating conflicting roles of VCAM-1 with the potential angiogenic role evidenced in several studies [22,23]. Interestingly, we saw a strongly potentiated response of VCAM-1 expression compared to ICAM-1 expression in hCMEC/D3 cells, therefore we speculate that they may be regulated by different regulatory mechanisms. In line with this, we did not observe a potentiation of IL-8 on hCMEC/D3 cells seeded on LM-10, which would suggest that it is not just an overall increased inflammatory profile when cells are seeded on LM-10, but a specific response dictated by the differential upregulation of selective adhesion molecules.

We next sought to determine the signalling mechanisms by which LM-10 may modulate the inflammatory activation of endothelial cells. Previous studies have shown a novel regulatory mechanism by which the ECM modulates ERK1/2 signalling after IL-1β treatment in rat astrocytes and rat brain endothelial cells *in vitro* [6,7]. However, IL-1β treatment failed to induce ERK1/2 and p38 MAPK pathways in hCMEC/D3 cells,

and therefore no effect of LM-10 was observed. Lack of effect of IL-1β treatment on ERK1/2 in endothelial has already been shown previously [3], however our results are contradictory to those reported by Ni and colleagues [24] who detected an increase in phospho-p38α in response to IL-1β treatment. In contrast, IL-1β treatment transiently activated NF-kB, a response previously observed by us in rat endothelial cell culture [7], and IL-1β-induced NF-kB activation was further potentiated by LM-10, suggesting that NF-kB activation may regulate IL-1β-induced adhesion molecule expression in hCMEC/D3 cells. In contrast our study demonstrates for the first time that regulation of IL-1-induced endothelial cell activation by LM-10 may be mediated by the YAP pathway, a recently described new signalling pathway shown to have critical roles in vascular systems, contributing to vessel homeostasis, vascular development, angiogenesis [25]. Specifically, we demonstrate here a novel temporal pattern of YAP phosphorylation at S127 and S397 regulated by IL-1 and LM-10. The subcellular distribution of YAP is controlled by the reversible phosphorylation of S127, resulting in binding and cytoplasmic retention, hence the inability to bind to TEADs [13,14], whilst the phosphorylation of S397 creates a phospho-degron motif for β-TrCP binding resulting in proteasomal degradation, providing an irreversible longer-term mechanism of YAP inhibition [15]. After IL-1β treatment in hCMEC/D3 cells, a similar decrease in pYAP(S127) followed by an increase back to respective basal levels was observed in cells on Matrigel and LM-10, whereas the temporal pattern of pYAP(S397) phosphorylation after IL-1β treatment was significantly impaired in cells on LM-10 compared to Matrigel. These findings suggest that IL-1β -induced phosphorylation of YAP at S127 and S397 is coupled when cells are seeded on Matrigel, whilst the phosphorylation of S127 and S397 is uncoupled in cells on LM-10, and that transient reductions in pYAP(127) and pYAP(397) on LM-10 are indicative of longer dephosphorylation of YAP, and hence translocation into the nucleus. In support of this, we show heavily decreased levels of Ctgf mRNA in hCMEC/D3 cells on matrigel 2 h after IL-1β treatment, reflective of decreased activation of genes downstream of YAP. In comparison, no significant change in Ctgf mRNA was observed 2 h after IL-1β treatment in hCMEC/D3 cells on LM-10, supporting our previous findings that YAP was not sequestered and degraded to the same degree in cells on Matrigel. However, we did not detect any significant change in Serpine1 mRNA levels. Since Serpine1 is typically associated with mechano-signalling [26], it is likely that this gene is not regulated via YAP in hCMEC/D3 cells after IL-1β treatment.

Conclusion

In conclusion, we demonstrate here for the first time a novel signalling mechanism whereby YAP signalling pathway is critically regulated by IL-1β and LM-10 in endothelial cells, providing new signalling mechanisms of cerebrovascular activation regulated by IL-1 and the ECM that could be targeted for the treatment of inflammatory CNS disease.

Abbreviations

BBB, blood-brain-barrier; BSA, bovine serum albumin; CNS, central nervous system; ECM, extracellular matrix; ELISA, enzyme-linked immunosorbent assay; ERK1/2, extracellular-regulated kinase 1/2, ICAM-1,

intercellular cell adhesion molecule-1; IL, interleukin; LM-10, laminin-10; NF-κB, nuclear factor kappa B, PBS, phosphate-buffered saline; qPCR, quantitative polymerase chain reaction; RT, room temperature; VCAM-1, vascular cell adhesion molecule-1

Declarations

Ethics approval and consent to participate

Not applicable

Consent for publication

All authors consent to the publication of this study

Availability of data and materials

All raw data and microscopy images are available upon request to the corresponding author

Competing interests

The authors have no competing interests

Funding

This work was funded by the British Heart Foundation (U.K.) studentship FS/17/6/32616

Authors' contributions

EP and JP obtained funding, formulated the original hypotheses, and designed the project. HT and EP designed the experiments. HT performed all experiments, analysed data and generated all the figures. HT, EP and JP wrote the manuscript.

Acknowledgements

Not applicable

References

1. Wang Q, Tang XN, Yenari MA. The inflammatory response in stroke. J Neuroimmunol. 2007;184:53–68.
2. Lu P, Takai K, Weaver VM, Werb Z. Extracellular matrix degradation and remodeling in development and disease. Cold Spring Harb Perspect Biol [Internet]. 2011;3:1–24.
3. Thornton P, W. McColl B, Cooper L, J. Rothwell N, M. Allan S. Interleukin-1 Drives Cerebrovascular Inflammation via MAP Kinase-Independent Pathways. Curr Neurovasc Res

4. Denes A, Pinteaux E, Rothwell NJ, Allan SM. Interleukin-1 and stroke: Biomarker, harbinger of damage, and therapeutic target. Cerebrovasc Dis. 2011;32:517–27.
5. Rodriguez-Grande B, Varghese L, Molina-Holgado F, Rajkovic O, Garlanda C, Denes A, et al. Pentraxin 3 mediates neurogenesis and angiogenesis after cerebral ischaemia. J Neuroinflammation. 2015;12:1–11.
6. Summers L, Kangwantas K, Nguyen L, Kielty C, Pinteaux E. Adhesion to the extracellular matrix is required for interleukin-1 beta actions leading to reactive phenotype in rat astrocytes. Mol Cell Neurosci. 2010;44:272–81.
7. Summers L, Kangwantas K, Rodriguez-Grande B, Denes A, Penny J, Kielty C, et al. Activation of brain endothelial cells by interleukin-1 is regulated by the extracellular matrix after acute brain injury. Mol Cell Neurosci. 2013;57:93–103.
8. Kangwantas K, Pinteaux E, Penny J. The extracellular matrix protein laminin-10 promotes blood–brain barrier repair after hypoxia and inflammation in vitro. J Neuroinflammation [Internet]. Journal of Neuroinflammation; 2016;13:25.
9. Warren JSA, Xiao Y, Lamar JM. YAP/TAZ activation as a target for treating metastatic cancer. Cancers (Basel). 2018;10.
10. Wang S, Zhou L, Ling L, Meng X, Chu F, Zhang S, et al. The Crosstalk Between Hippo-YAP Pathway and Innate Immunity. Front Immunol. 2020;11:1–14.
11. Choi H-J, Kim N-E, Kim B, Seo M, Heo J. TNF-α-Induced YAP/TAZ Activity Mediates Leukocyte-Endothelial Adhesion by Regulating VCAM1 Expression in Endothelial Cells. Int J Mol Sci. 2018;19:3428.
12. Weksler B, Romero IA, Couraud PO. The hCMEC/D3 cell line as a model of the human blood brain barrier. Fluids Barriers CNS [Internet]. Fluids and Barriers of the CNS; 2013;10:1.
13. Zhao B, Wei X, Li W, Udan RS, Yang Q, Kim J, et al. Inactivation of YAP oncoprotein by the Hippo pathway is involved in cell contact inhibition and tissue growth control. Genes Dev. 2007;21:2747–61.
14. Zhao B, Ye X, Yu J, Li L, Li W, Li S, et al. TEAD mediates YAP-dependent gene induction and growth control. Genes Dev. 2008;22:1962–71.
15. Zhao B, Li L, Tumaneng K, Wang CY, Guan KL. A coordinated phosphorylation by Lats and CK1 regulates YAP stability through SCFβ-TRCP. Genes Dev. 2010;24:72–85.
16. Burnside ER, Bradbury EJ. Review: Manipulating the extracellular matrix and its role in brain and spinal cord plasticity and repair. Neuropathol Appl Neurobiol. 2014;40:26–59.
17. Indyk JA, Chen ZL, Tsirka SE, Strickland S. Laminin chain expression suggests that laminin-10 is a major isoform in the mouse hippocampus and is degraded by the tissue plasminogen activator/plasmin protease cascade during excitotoxic injury. Neuroscience. 2003;116:359–71.
18. DeCicco-Skinner KL, Henry GH, Cataisson C, Tabib T, Curtis Gwilliam J, Watson NJ, et al. Endothelial cell tube formation assay for the in vitro study of angiogenesis. J Vis Exp. 2014;10:1–8.

19. Radisavljevic Z, Avraham H, Avraham S. Vascular endothelial growth factor up-regulates ICAM-1 expression via the phosphatidylinositol 3 OH-kinase/AKT/nitric oxide pathway and modulates migration of brain microvascular endothelial cells. J Biol Chem. 2000;275:20770–4.
20. Ucuzian AA, Gassman AA, East AT, Greisler HP. Molecular mediators of angiogenesis. J Burn Care Res. 2011;31:158–75.
21. Kasselman LJ, Kintner J, Sideris A, Pasnikowski E, Krellman JW, Shah S, et al. Dexamethasone treatment and ICAM-1 deficiency impair VEGF-induced angiogenesis in adult brain. J Vasc Res. 2007;44:283–91.
22. Gao D, Nolan DJ, Mellick AS, Bambino K, McDonnell K, Mittal V. Endothelial Progenitor Cells Control the Angiogenic Switch in Mouse Lung Metastasis. Science. 2008;319:195–8. Available from: http://www.sciencemag.org/cgi/doi/10.1126/science.1150224
23. Kang Z, Zhu H, Luan H, Han F, Jiang W. Curculigoside A induces angiogenesis through VCAM-1/Egr-3/CREB/VEGF signaling pathway. Neuroscience. 2014;267:232–40.
24. Ni Y, Teng T, Li R, Simonyi A, Sun GY, Lee JC. TNFα alters occludin and cerebral endothelial permeability: Role of p38MAPK. PLoS One. 2017;12:1–20.
25. Park JA, Kwon YG. Hippo-YAP/TAZ signaling in angiogenesis. BMB Rep. 2018;51:157–62.
26. Liu F, Lagares D, Choi KM, Stopfer L, Marinković A, Vrbanac V, et al. Mechanosignaling through YAP and TAZ drives fibroblast activation and fibrosis. Am J Physiol - Lung Cell Mol Physiol. 2015;308:L344–57.

Figures

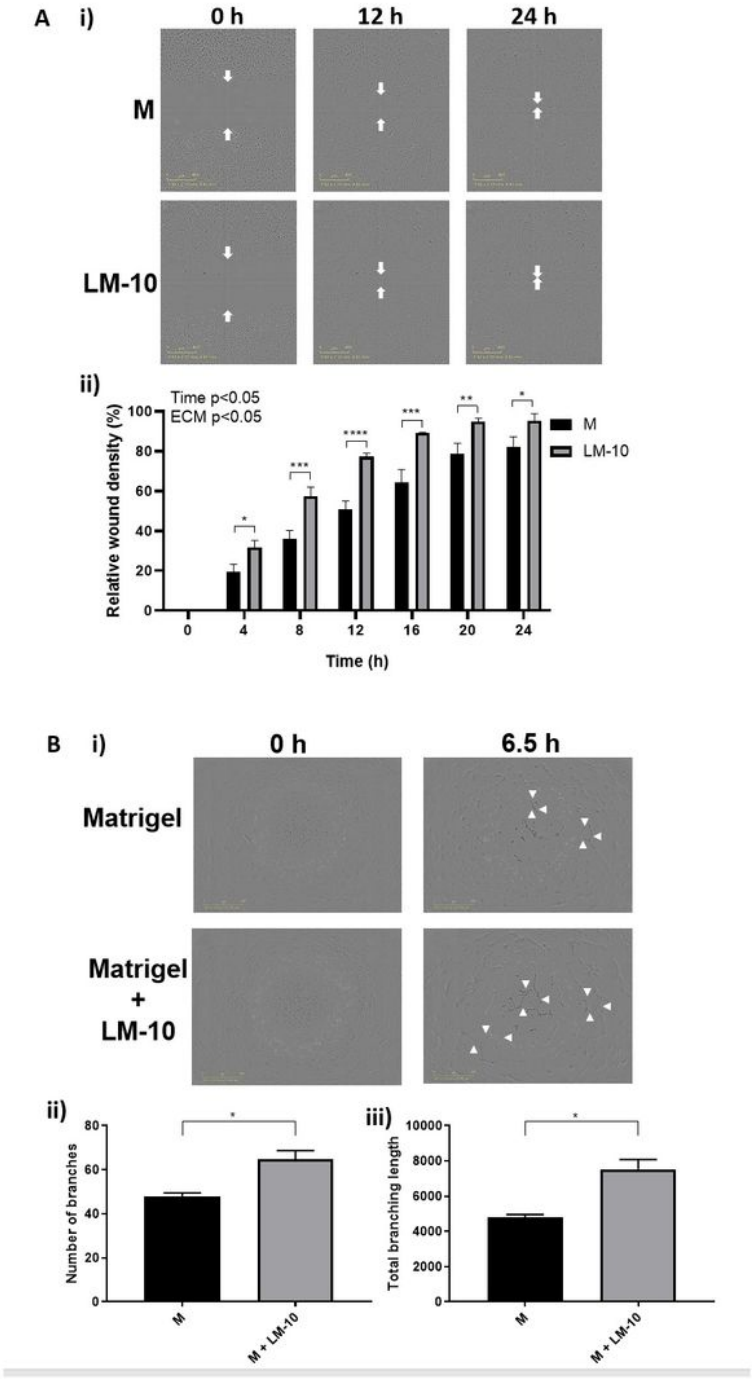

Figure 1

Effect of LM-10 on hCMEC/D3 cell migration and cell tube formation. (Ai) Representative images and (Aii) quantification of the scratch assay. 96-well Essen ImageLock plates were pre-coated with Matrigel (20 µg/ml) or LM-10 (10 µg/ml). 40,000 hCMEC/D3 cells were seeded for 4 h and the 96-pin IncuCyte WoundMaker Tool was used to create uniform cell-free zones. Phase contrast images were acquired every 4 h on an Incucyte Zoom Live Cell Analysis system using a 123 4x/3.05 Plan Apo OFN25 objective.

Arrows indicate boundaries of the scratched regions. Scale bar 400 µm. The Incucyte scratch wound assay analysis software as used to calculate relative wound confluence. (Bi) Representative images and quantification (Bii-iii) of the tube formation assay. 96-well plates were pre-coated with Matrigel (9.16 mg/ml) or Matrigel (9.16 mg/ml) supplemented with LM-10 (10 µg/ml). 10,000 hCMEC/D3 cells were seeded on top of the Matrigel layer. Phase contrast images were acquired at 0 and 6.5 h on an Incucyte Zoom Live Cell Analysis system (Essen BioScience, UK) using a 123 4x/3.05 Plan Apo OFN25 objective. Scale bar 800 µm. The angiogenesis analyser macro in ImageJ was used to quantify number of branches (Bii) and total branching length (Biii). Data are represented as mean ± SEM of 3 technical replicates and 3 biological replicates (n=3, A) and of 2 technical replicates and 4 biological replicates (n=4, B). Data were assessed by a two-way RM ANOVA followed by Sidak's post-hoc analysis comparing the means of wound confluence at corresponding time points on Matrigel vs LM-10 (A). Significant main effects of time and the ECM coating are indicated on the top left of the graphs (A). Data were assessed by paired t-test to compare coatings (B). *p<0.05, **p<0.01, ***p<0.001, ****p<0.0001.

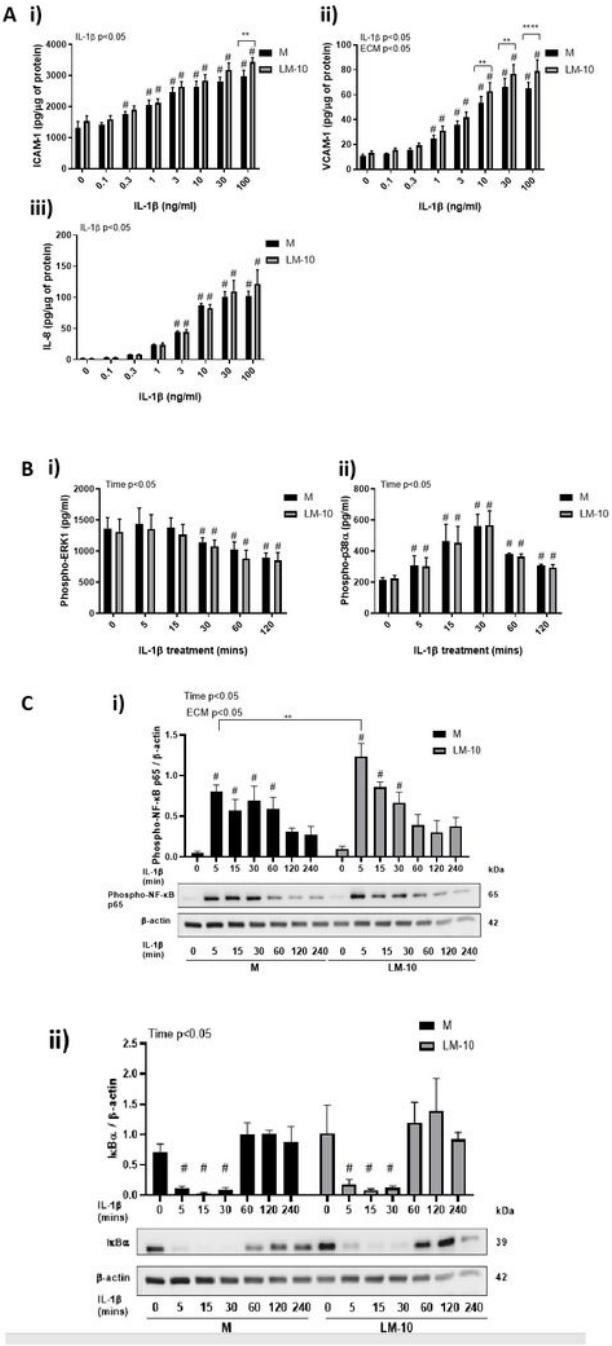

Figure 2

Effect of LM-10 on IL-1β-induced activation in hCMEC/D3 cells and IL-1β signalling pathways. (Ai-iii) hCMEC/D3 cells seeded at a density of 200,000 cells/well in a 24-well plate for 4 h were treated with IL-1β at various concentrations for 24 h. Cell supernatants and lysates were assayed for ICAM-1 (Ai), VCAM-1 (Aii) or IL-8 (Aiii) by ELISA. (Bi-ii) hCMEC/D3 cells were treated with 10 ng/ml of IL-1β for various times, and cell lysates were assayed for phospho-p38α (Bi) and phospho-ERK1/2 (Bii) by ELISA. (Ci-ii)

hCMEC/D3 cells were treated with IL-1β (10 ng/ml) for various times, and cell lysates were assayed for phospho-NF-κB p65 (Ci) and IκBα (Cii) by Western blot. Phospho-NF-κB p65, IκBα and β-actin were quantified using densitometry on ImageJ. Phospho-NF-κB p65 and IκBα were normalised to β-actin and the ratio is presented. Data are represented as mean ± SEM of 4 biological replicates, and were analysed by a two-way RM ANOVA followed by Sidak's post-hoc analysis comparing the means of expression of adhesion molecule/cytokine at corresponding concentrations of IL-1β treatment on Matrigel vs LM-10 and comparing the means of signalling molecules at corresponding time points on Matrigel vs LM-10, # represents significance within ECM to untreated (A). Significant main effects of IL-1β treatment and the ECM coating are indicated on the top left of the graphs (A). Data were assessed by a two-way RM ANOVA followed by Sidak's post-hoc analysis comparing the means of signalling molecules at corresponding time points on Matrigel vs LM-10, # represents significance within ECM to untreated (B-C). Significant main effects of IL-1β treatment time and the ECM coating are indicated on the top left of the graphs (B-C). *p<0.05, **p<0.01, ***p<0.001, ****p<0.0001.

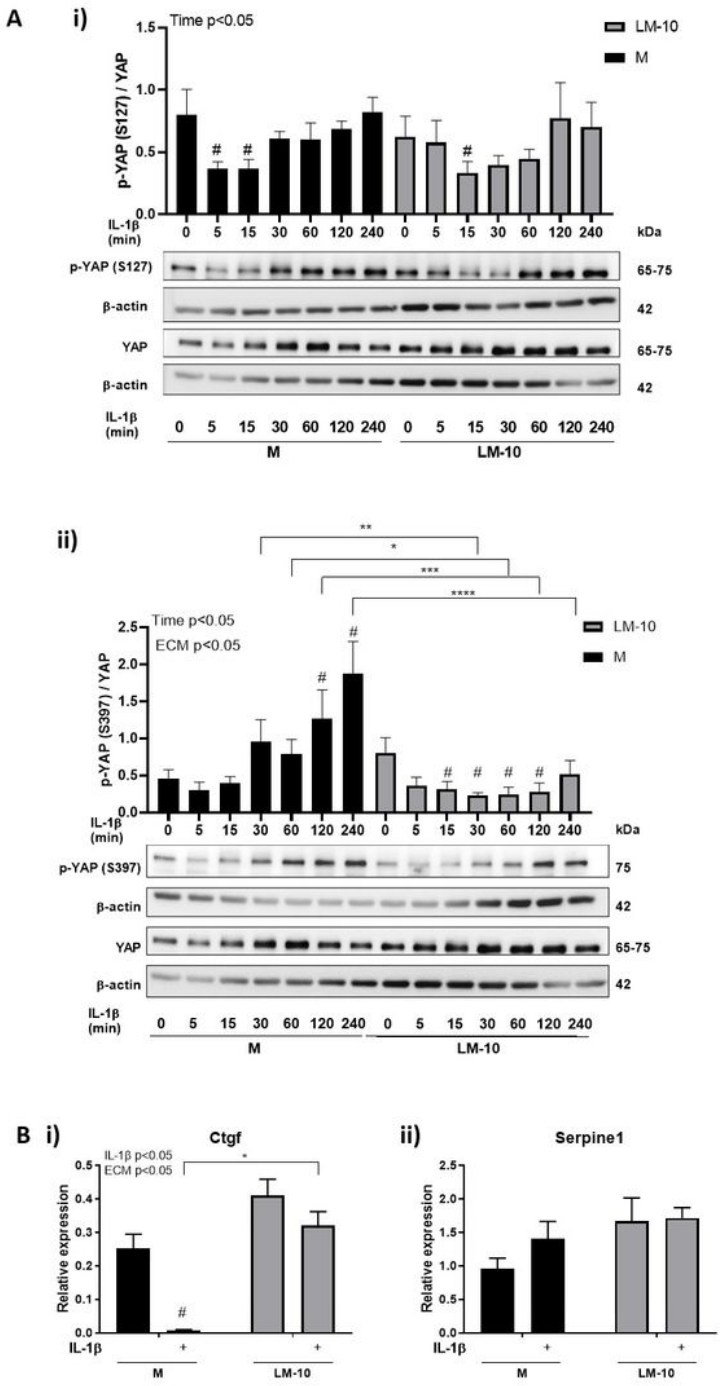

Figure 3

Effect of LM-10 on YAP signalling after IL-1β-induced activation in hCMEC/D3 cells and on genes expression downstream of YAP. (Ai-ii) hCMEC/D3 cells were seeded at a density of 200,000 cells/well in a 24-well plate for 4 h. Cells were treated with IL-1β (10 ng/ml) for various length of time (from 5 min to 240 min). Cell lysates were then collected and assayed for p-YAP(S127), p-YAP(S397) and total YAP by Western blot. p-YAP(S127), p-YAP(S397), YAP and β-actin were quantified using densitometry on ImageJ.

p-YAP(S127), p-YAP(S397) and YAP were normalised to β-actin, and the ratio of normalised p-YAP (S127)/total YAP and p-YAP (S397)/total YAP was calculated. (Bi-ii) hCMEC/D3 cells were treated with IL-1β (10 ng/ml) for 2 h. Cell lysates were collected and mRNA levels (normalised to GAPDH housekeeping control) of Ctgf (Bi) and Serpine 1 (Bii) were assayed by qPCR. Data are represented as mean ± SEM of 4 biological replicates (n=4, A-B). The blots are representative images (A). Data were assessed by a two-way RM ANOVA followed by Sidak's post-hoc analysis (A). *represents significance comparing the mean ratio of p-YAP(S127)/total YAP at corresponding time points on Matrigel vs LM-10 and # represents significance within ECM to baseline (A). Significant main effects of IL-1β treatment time and the ECM coating are indicated on the top left of the graphs (A). * Data were assessed by a two-way RM ANOVA followed by Sidak's post-hoc analysis, * represents significance between corresponding conditions on Matrigel vs LM-10 and # represents significance within ECM to baseline (B). Significant main effects of IL-1β treatment and the ECM coating are indicated on the top left of the graphs (B). *$p<0.05$, **$p<0.01$, ***$p<0.001$, ****$p<0.0001$.